A Comparison of the AC and DC Power Flow Models for LMP Calculations

Thomas J. Overbye, Xu Cheng, Yan Sun
Department of Electrical and Computer Engineering
University of Illinois at Urbana-Champaign
Urbana, IL 61801 USA
overbye@ece.uiuc.edu, xucheng@students.uiuc.edu, yansun@students.uiuc.edu

Abstract

The paper examines the tradeoffs between using a full ac model versus the less exact, but much faster, dc power flow model for LMP-based market calculations. The paper first provides a general discussion of the approximations associated with using a dc model, with an emphasis on the impact these approximations will have on security constrained OPF (SCOPF) results and LMP values. Then, since the impact of the approximations can be quite system specific, the paper provides case studies using both a small 37 bus system and a somewhat larger 12,965 bus model of the Midwest U.S. transmission grid. Results are provided comparing both the accuracy and the computational requirements of the two models. The general conclusion is that while there is some loss of accuracy using the dc approximation, the results actually match fairly closely with the full ac solution.

1. Introduction

The most accurate approach for modeling the steady-state behavior of balanced, three phase, electric power transmission networks is through the solution of the power flow. From the power flow solution, which contains the voltage magnitude and phase angles at each bus in the system, all other values can be derived, including the real and reactive flows on all the lines in the system. The power flow, which requires the iterative solution of a set of nonlinear algebraic equations, is typically taught in the junior or senior year of an electric power engineering curriculum. It is also considered the most heavily used tool by power system engineers. With modern computers the power flow for even a fairly large system, such as the NERC 43,000 bus model of the North American Eastern Interconnect, can often be solved in seconds.

However, a "secret" well-known to practicing engineers is the power flow solution can often be maddeningly difficult to obtain, particularly when a good initial guess of the solution is not available. The "flat start" starting point taught to undergraduates for small systems rarely works when solving large, realistic systems. These convergence problems are especially troublesome when one tries to substantially change the operating point for a previously solved case, such as by scaling the load/generation levels.

There are several reasons for these solution difficulties. First, the nonlinear power balance equations themselves usually have a large number of alternative (low voltage) solutions, or, more rarely, no solution [1]. So even when the power flow converges it may not have found the desired solution. Second, when using the common Newton-Raphson method the region of convergence for these solutions, including the desired high-voltage solution, is fractal [2], [3], [4]. For stressed systems a "reasonable" initial guess might actually be in the region of convergence of a low voltage solution. Third, the power flow algorithm must not only solve the nonlinear power balance equations, but it must often determine the correct values for large number of discrete and/or limited automatic controls. These controls values include generator AVR status, LTC and phase shifting transformer tap positions, discrete switched shunt reactive compensation values, the power flow on direct current (DC) lines, and more recently the values for FACTS devices. Further complicating the situation, the series impedance of the LTC and phase shifting transformers is often dependent upon the transformer's tap value. Last, the power flow models themselves are often "hard-coded" for a specified operating point. This hard-coding is particularly apparent with the values of fixed reactive shunts at buses, which usually represent manually switched capacitors, but is also apparent in the control settings for other devices such as phase shifting and LTC transformers, and generator voltage setpoint values. For example, scaling down the load/generation for a peak case, and then trying to resolve can be very problematic since the large amount of fixed, primarily capacitive, compensation quickly results in abnormally high voltages.

In addition to convergence difficulties, solving the full power flow can be time consuming, particularly when a large number of contingencies need to be considered. While a single solution for a large system may solve in

seconds for a large case, the solution process rapidly becomes computationally bound when a large number of contingent systems need to be solved as well. For example, trying to solve all the single device outages for the 57,000 line 2002 Series NERC MMWG case would take many hours, even if each individual contingent power flow solved in a second. Of course, the contingency analysis problem is inherently parallel, so the availability of multiple processors could be of substantial benefit.

Given the difficulties in solving the full power flow, it is not surprising that many approximate methods have been proposed and used. An analytic study of many of these approximations is given in [5]. The focus of the present paper is to examine the accuracy tradeoffs between using the full power flow model versus the most dramatic of these approximate methods, the "dc power flow" [6], for LMP-based market calculations. The motivation for the present paper is the proliferation of market type studies with results based entirely on the dc power flow. This paper is not advocating the replacement of the power flow with a dc power flow for operational studies.

This paper is organized as follows. Section 2 provides a brief discussion of the dc power flow algorithm, while Section 3 contrasts the full security constrained OPF (SCOPF) with a dc implementation of the SCOPF. The remaining sections of the paper then provide case study results. Throughout the paper to differentiate between the two solution methodologies the full power flow/SCOPF results will be called the "ac" solution, while the dc power flow/SCOPF will be called the "dc" solution. Of course, both techniques are attempting to model the same underlying ac power system, and both techniques can accommodate HVDC transmission lines as well.

2. DC Power Flow and Contingency Analysis

The dc power flow greatly simplifies the power flow by making a number of approximations including 1) completely ignoring the reactive power balance equations, 2) assuming all voltage magnitudes are identically one per unit, 3) ignoring line losses, and 4) ignoring tap dependence in the transformer reactances. Hence the dc power flow reduces the power flow problem to a set of linear equations

$$\mathbf{P} = \mathbf{B'}\ \boldsymbol{\theta} \tag{1}$$

where $\mathbf{P}$ is the vector of bus real power injections, $\mathbf{B'}$ is bus susceptance matrix, and $\boldsymbol{\theta}$ is the vector of bus voltage angles. Since the equations are linear they always have a single solution, which can be directly calculated by solving

$$\boldsymbol{\theta} = [\mathbf{B'}]^{-1}\ \mathbf{P} \tag{2}$$

eliminating the need for iterations.

How well the dc power flow solution approximates the actual power flow solution depends, of course, upon the power system. It is easy to conceive of cases in which the results are identical, such as a two bus system with generators at each bus, regulating their terminal to 1.0 per unit with their reactive power limits, connected through a lossless transmission line. It is likewise easy to conceive of cases in which the dc power flow results are completely wrong. For example, a two bus system with a generator at one end and a constant power load at the other end with a value greater than the system's maximum loadability – the dc power flow will indicate a normal solution, while the actual power flow equations to not have a solution [7]. While techniques such as those in [5] can be helpful for smaller systems, for large systems it is very difficult to analytically quantify the errors introduced with the dc power flow. The approach of this paper is to present case specific examples.

Before moving on it is important to point out that one of the most obvious differences between the two – the lack of losses in the dc solution – can be reasonably compensated for by increasing the total dc load by the amount of the ac losses. Hence, in the dc approach the estimated transmission system losses could be allocated to the bus loads. This requirement to first estimate the losses is usually not burdensome since the specified total control area "load" is actually the true load plus the losses. Indeed, the control area total loads given in the U.S. FERC Form 714 filings are actually load plus losses. Therefore in attempting to duplicate the Form 714 load values with a full power flow the true load must be estimated by taking the reported load and subtracting off the estimated losses. In this paper when comparing the ac and dc solution results the dc solution load value has first been increased to match the total ac load plus losses.

Computationally the dc power flow has at least three advantages over the standard Newton-Raphson power flow. First, by just solving the real power balance equations its equation set is about half the size of the full problem. Second, the dc power flow is noniterative, requiring just a single solution of (2). Third, because the $\mathbf{B'}$ matrix is state-independent provided the system topology does not change it need only be factored once. Therefore one would expect the dc power flow to be about ten times faster than the regular power flow for the initial solution, and even faster for subsequent solutions since solving for $\boldsymbol{\theta}$ with a modified $\mathbf{P}$ would only require a forward/backward substitution.

For contingency analysis the computational speedups available by using linear approximations are even more dramatic. Linear methods for contingency analysis have been used for many years [8], [9]. In the line outage distribution factor (LODF) approach [6] the affects of

single and multiple device outages can be linearly approximately by calculating the state-independent LODF

$$d_{l,k} = \frac{\Delta f_l}{f_k^0} \tag{3}$$

where Δf_l is the change in MW flow on line l following the outage of line k, and f_k^0 is the original flow on line k before it was outaged. The LODF vector $\mathbf{d}_k$ contains the LODFs for all monitored lines. Similar values can also be calculated for line closure contingencies. Since the LODFs are state independent they can be calculated once and used many times for contingency analysis. Once the factored **B'** matrix is available, the computation requirements to calculate each LPDF vector are proportional to a fast forward/full backward substitution. This allows the contingencies to be linearly approximated many times faster than the approach of actually solving the power flow for the contingent system.

3. Full AC and DC LP-Based SCOPF

The OPF algorithm, which was first formulated in the 1960's [10], [11], involves the minimization of some objective function subject to a number of equality and inequality constraints:

$$\begin{aligned} &\text{Minimize } F(\mathbf{x},\mathbf{u}) \\ &\text{s.t. } \mathbf{g}(\mathbf{x},\mathbf{u}) = \mathbf{0} \\ &\mathbf{h}_{\min} \le \mathbf{h}(\mathbf{x},\mathbf{u}) \le \mathbf{h}_{\max} \\ &\mathbf{u}_{\min} \le \mathbf{u} \le \mathbf{u}_{\max} \end{aligned} \tag{4}$$

where **x** is a vector of the dependent variables (such as the bus voltage magnitudes and angles), **u** is a vector of the control variables, F(**x**,**u**) is the scalar objective function, **g**(**x**,**u**) is the set of equality constraints (e.g., the power flow equations), and **h**(**x**,**u**) is the set of inequality constraints.

Originally, the OPF only considered base case violations, but was later augmented to include contingency constraints in a formulation now know as the security constrained OPF (SCOPF) [12], [13], [14]. Over the years several different OPF and SCOPF solution approaches have been proposed, with an excellent literature survey recently presented in [15] and a tutorial in [16]. These approaches can be broadly classified as either linear programming (LP) based methods or non-linear programming based methods. The algorithm utilized here is based upon the LP approach [17].

Overall, the LP SCOPF implemented here iterates between solving the power flow and contingency analysis to determine the power system violations, with an LP with a linearized model of system constraints to redispatch the control variables subject to certain equality and inequality constraints. This "outer loop" iteration requires that following any control changes contingency analysis by rerun to insure the control changes did not introduce any new contingent violations. Usually two or three outer loop iterations are required.

The key to the computational efficiency of the LP itself is to minimize the number of constraints included in the LP tableau. Practically all the constraints of (4) are considered by either enforcing them using the power flow/contingency analysis, or, in the case of most nonbonding inequality constraints, monitoring but not enforcing them as long as they remain nonbonding. The difference between the ac and dc approaches is only in the power flow and contingency analysis calculations. The remainder of the algorithm is the same.

For the main optimization the LP itself utilizes a primal simplex algorithm with explicitly bounded variables [18]:

$$\begin{aligned} &\text{Minimize } \mathbf{c}^T\mathbf{u} \\ &\text{s.t. } \mathbf{A}\mathbf{u} = \mathbf{b} \\ &\mathbf{u}_{\min} \le \mathbf{u} \le \mathbf{u}_{\max} \end{aligned} \tag{5}$$

where **u** is the vector of control variables from (4) augmented to include the LP slack variables, **c** is the vector of the current control incremental costs, **A** contains the active linearized constraints, and **b** is the vector of limit violations. Lack of feasibility is handled using the slack variable approach of [19]. The elements of each row in **A** can be calculated quite efficiently either using the approach from [20] for the ac solution, or from the LODFs for the dc approach.

Once an optimal solution has been determined, the marginal costs for enforcing the different constraints can be determined from the control costs and the final LP basis matrix:

$$\boldsymbol{\lambda}^T = \mathbf{c}_B^T \mathbf{A}_B^{-1} \tag{6}$$

where

$\boldsymbol{\lambda}^T$ = marginal costs of enforcing constraints
$\mathbf{c}_B^T$ = control costs
$\mathbf{A}_B$ = LP basis matrix

The bus MW marginal costs (also known as the locational marginal prices or LMPs) are then computed as

$$\boldsymbol{\lambda}_{buses}^T = \boldsymbol{\lambda}^T \mathbf{S} \tag{7}$$

where

$\boldsymbol{\lambda}_{buses}^T$ = bus MW marginal costs

S = matrix of sensitivity of bus MW injections to the set of constraints

It should be emphasized that the bus LMPs are strictly a function of the binding constraints. Other potential constraints, such as a line with a flow of 99.9% of its limit, will have no impact. But once a constraint becomes binding it will have a discrete, potentially large, impact on the bus LMPs. Hence in doing a comparison of the ac and dc SCOPFs, it must be kept in mind that large LMP differences do not necessarily indicate large deviations in the power system solutions.

3. Thirty-Seven Bus System Case Study

The first test system is based upon the 37 bus, nine generator, 58 transmission line/transformer (line) power system used for the final ac SCOPF solution presented in [21]. This system was modified slightly for use here by 1) adding two additional high priced generators to avoid unenforceable SCOPF solutions are higher load levels, 2) through the removal of a small amount of real power shunts, and 3) by balancing the taps at two of the 138/69 kV transformers to correct a circulating var problem. A one-line of this system is shown in Figure 1, while Figure 2 shows the supply curve. The size of the green arrows in Figure 1 are proportional to the MW flow on each of the lines, while the pie charts show the percentage loading of each line.

This system has four 345 kV buses, eleven 138 kV buses and 22 69 kV buses. The average r/x ratio for the transmission lines and transformers in the system, which was derived from an actual power grid, is 0.38, with a high of 1.82 (for an underground cable) and a low of 0.016 (for a 345/138 kV transformer). The contingency set consisted of the 58 single line outages. The base case, which corresponds to the SCOPF solution from [21], had a load of 832.9 MW and 286.2 Mvar, and losses of 12.0 MW. The per unit voltages ranged between 0.993 and 1.032 per unit. The ac SCOPF solution contains a single binding contingent constraint – the MVA flow on the Pete69 to UIUC69 kV line is binding at its limit of 93 MVA for the contingent loss of the Tim69 to Hisky69 kV line. The marginal cost for this constraint is $22.20 / MVA-hr.

As an initial comparison of the dc power flow results with the ac results, the bus loads for the dc system were scaled uniformly to increase the load system load of 844.9 MW (i.e., load + losses for the ac system). The dc SCOPF was then solved. A comparison of the MVA line flows from the ac solution with the MW line flows from the dc solution revealed very good correspondence for most lines, with all but two of the differences below 10 MVA and all but four below 5 MVA. The two large discrepancies were both on lines with high reactive power flow and low real power flow. Since the dc approach ignores reactive power flow it can't match flows real when the flow is primarily reactive. Even with these two large errors the average of the absolute value of the 58 line flow errors is just 2.3 MVA, with an average flow of 49.4 MVA so the error is about 4.6%. If the comparison is just between the MW flows the absolute value of the error is just 1.25 MW with a high of 4.6 MW.

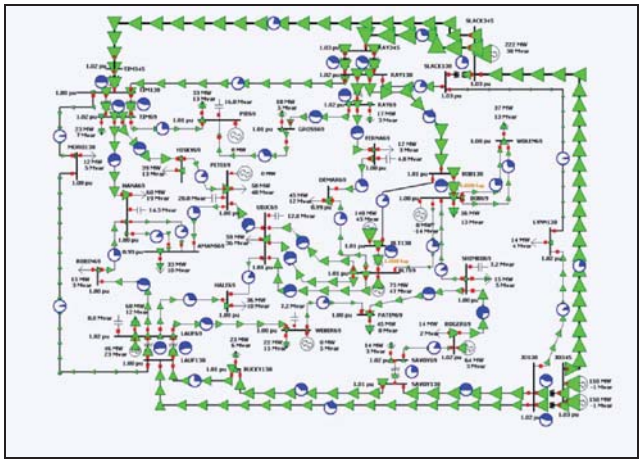

Figure 1: 37 Bus System One-line Diagram

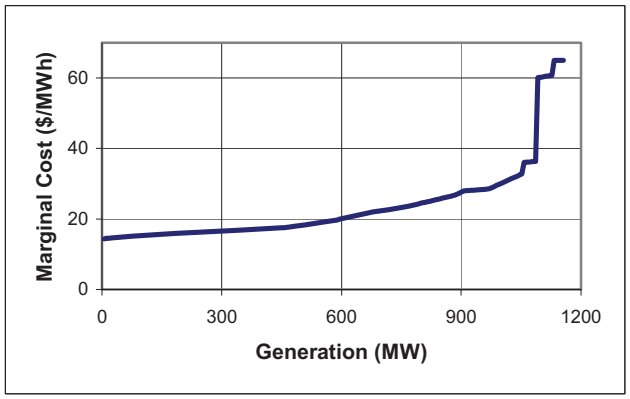

Figure 2: 37 Bus Case Generator Supply Curve

The dc SCOPF solution contained the same single binding constraint as the ac solution, albeit with a somewhat different marginal cost, $18.63/MVA-hr, compared to $22.20/MVA-hr for the ac solution. A comparison of the resultant ac and dc bus LMPs showed fairly close agreement. The ac LMP was $ 27.88/MWh, while the average dc LMP was $27.57, a difference of just slightly more than 1%. The largest deviations, $2.88/MWh and $2.79/MWh, were at the buses adjacent to the binding constraint.

Next, for a more comprehensive comparison, the system load was uniformly increased in 2 MW increments from an initial load of 750 MW (the point at which congestion begin to appear in the ac solution) to 1000

MW, with the SCOPF solved at each point. Hence a total of 126 SCOPFs were solved. A similar scaling was done with the dc SCOPF, except as the system load was increased slightly to compensate for losses. A comparison was then done, both in terms of how well the dc SCOPF found the same binding constraints as the ac SCOPF, and in terms of how well the bus LMPs matched.

Table 1 and Table 2 provide a comparison of the binding line/contingency pairs, with the first two columns showing the line from and to bus, the third showing the single line contingency that caused the constraint, and the last column showing the number of solutions for which this line/contingency was a binding constraint (out of 126). Note, each line was only binding for a single contingency and each contingency only had at most one binding line. Overall, the dc SCOPF correctly determined 5 out of the 6 binding line/contingency pairs, and 77% (254 out of 330) of the total binding constraints. Also, it is not surprising the ac solution found more binding constraints than the dc solution, given that the ac solution is enforcing MVA constraints, which are always at least as large as the underlying MW flow enforced by the dc solution, and usually larger whenever the reactive flow is nonzero. One simple approach for increasing the accuracy of the dc SCOPF might be to use fast techniques, such as the one presented in [22], to estimate this reactive flow.

Table 1: AC Binding Device Summary

From Bus	To Bus	Contingency	# Binding
TIM69	PIE69	RAY69-RAY138	37
UIUC69	PETE69	TIM69-HISKY69	100
AMANS69	PETE69	TIM69-HANA69	44
SHIMKO69	PATEN69	WEBER69-LAUF69	52
SHIMKO69	ROGER69	BUCKY138-SAVOY138	77
LAUF69	LAUF138	LAUF69-LAUF138	20

As for the LMPs, Table 3 compares the average values for the 126 points. Notice that overall the agreement is quite good, but that there are some significant deviations at individual buses. To give a feel for the variation in the individual LMPs Figure 3 and Figure 4 show tabular contour plots of the ac and dc LMPs [23]. In each figure, the rows correspond to the 126 different system load values (i.e., from 750 to 100 MW in 2 MW increments), with the load increasing from the top. The columns then correspond to the buses, with the order from left to right as per Table 3. The LMP values for each load level/bus are colored using the Figure 5 key. Note that while the individual LMPs differ between the ac and dc solutions, they do tend to follow the case general pattern.

Table 2: DC Binding Device Summary

From Bus	To Bus	Contingency	# Binding
TIM69	PIE69	RAY69-RAY138	4
UIUC69	PETE69	TIM69-HISKY69	91
AMANS69	PETE69	TIM69-HANA69	29
SHIMKO69	PATEN69	WEBER69-LAUF69	55
SHIMKO69	ROGER69	BUCKY138-SAVOY138	75

Table 3: LMP ($/MWh) Comparison for 37 Bus Case

Num.	Name	AC LMP	DC LMP	Diff.
1	TIM345	28.52	28.99	0.47
3	MORO138	29.48	29.94	0.45
5	ROBIN69	36.58	35.45	-1.13
10	RAY69	32.99	28.53	-4.46
12	TIM69	30.90	31.48	0.58
13	FERNA69	30.07	26.92	-3.15
14	WEBER69	30.97	30.65	-0.32
15	UIUC69	22.99	23.27	0.27
16	PETE69	50.29	47.39	-2.89
17	PIE69	37.70	31.07	-6.63
18	HANA69	43.02	40.88	-2.13
19	GROSS69	36.31	30.38	-5.94
20	SHIMKO69	26.55	26.53	-0.02
21	WOLEN69	25.02	24.97	-0.05
24	HALE69	24.65	24.67	0.02
27	HISKY69	50.39	47.42	-2.97
28	JO345	28.19	28.63	0.44
29	JO138	28.19	28.62	0.42
30	BUCKY138	28.58	28.93	0.36
31	SLACK345	28.20	28.64	0.44
32	SAVOY138	28.01	28.33	0.32
33	SAVOY69	27.17	27.23	0.06
34	PATEN69	29.92	29.70	-0.22
35	SLACK138	28.02	28.43	0.41
37	AMANS69	43.90	41.31	-2.59
38	RAY345	28.04	28.46	0.41
39	RAY138	27.69	28.04	0.35
40	TIM138	29.78	30.29	0.51
41	LAUF138	28.99	29.38	0.39
44	LAUF69	29.79	29.61	-0.18
47	BOB138	25.39	25.47	0.08
48	BOB69	25.04	24.97	-0.08
50	RODGER69	25.75	25.69	-0.05

53	BLT138	25.13	25.22	0.09
54	BLT69	23.38	23.42	0.04
55	DEMAR69	26.99	25.09	-1.89
56	LYNN138	28.12	28.54	0.42
	Average	**30.56**	**29.80**	**-0.76**

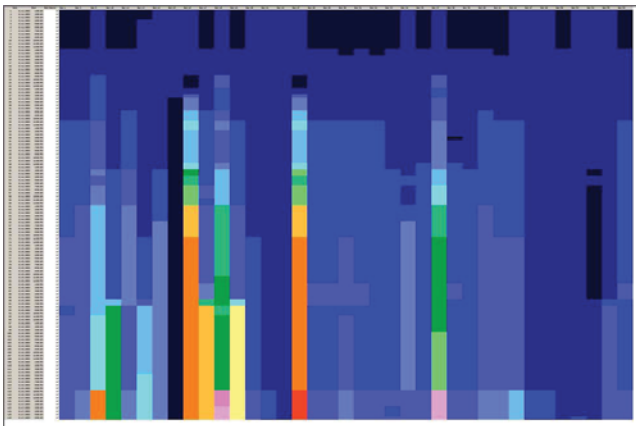

Figure 3: 37 Bus Load Variation Contour of the AC LMPs

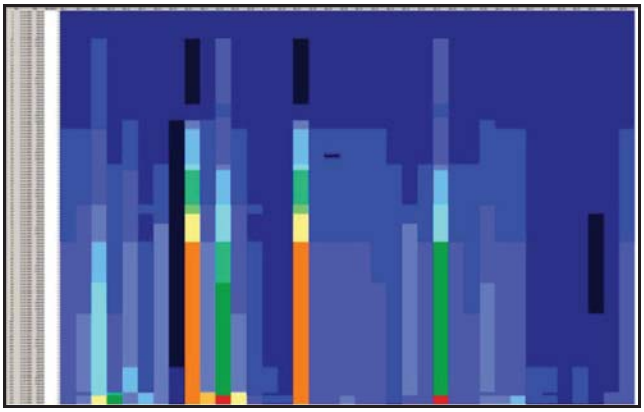

Figure 4: 37 Bus Load Variation Contour of the DC LMPs

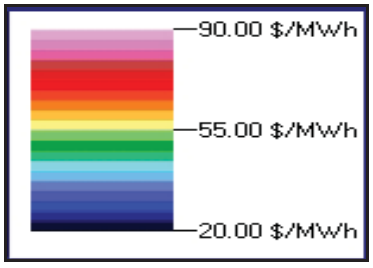

Figure 5: Color Key for Figure 3 and Figure 4

4. Midwest System Case Study

As a second, somewhat larger test system, the ac and dc SCOPFs were compared using a 12,925 bus, 1790 generator case derived from the 43,000 bus 2002 NERC/MMWG 2003 Summer Case. Since the focus area was the U.S. Midwest in general and Illinois in particular, the original case was equivalenced with the explicitly retained portion of the system roughly covering the region bounded by Minnesota, Missouri, Tennessee, Ohio and Michigan. Realistic cost estimates were determined for practically all the generators in the case. Figure 6 shows the system supply curve, with the assumption that all generators are available. The initial system load was 171.48 GW.

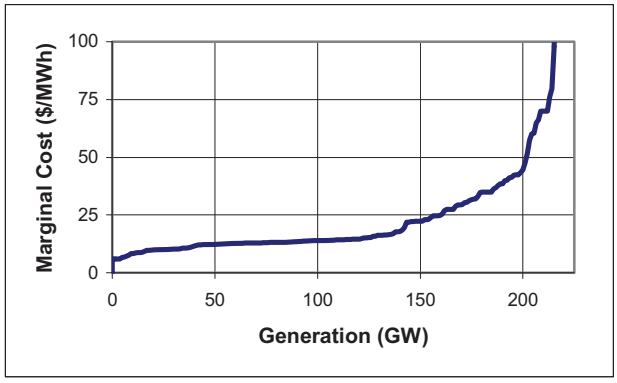

Figure 6 : Midwest System Supply Curve

For the SCOPF solution the entire system was treated as a single operating area with the flows on 4349 lines monitored and enforced if necessary. All generators were modeled as being available controls, as were eleven phase shifting transformers. In the ac system full impedance scaling was used with the phase shifting transformers, with the impedance generally ranging between 100% and 200% of the zero phase angle value. For the dc solution such state dependent impedance scaling was not used. Rather, the impedance values were fixed at the 0 phase angle value.

The contingency set consisted of 1360 contingencies, with about half the contingencies being single device outages, while the remainder had various combinations of device outages, insertions, and load moves; the most complicated contingency had 18 separate actions. As was the case with the 37 bus system, for the dc solution the total system load was uniformly increased to include the initial ac losses. The initial voltages for the ac system ranged between 0.866 and 1.430 per unit, with about 90 buses having voltages below 0.95 per unit, and 450 having voltages above 1.05 per unit.

To get a feel for the accuracy of the dc power flow solution, the dc power flow was solved using the base case ac power flow generation values, and then the MW and MVA flows on all 17,647 lines were compared. Overall the correspondence between the two was quite good, with an average of the absolute value of the difference between the dc MW and the ac MVA just 4.12 MW/MVA, compared to an average flow of 64.2 MVA. The highest

error of 396.8 MVA occurred on a branch connecting a large capacitor to the rest of the system and hence had an entirely reactive flow; the next largest error was 195 MVA. Overall 57 lines had errors at or above 100 MVA, 159 at or above 50 MVA, and 1675 at or above 10 MVA. If the comparison was just limited to MW flows the average error was just 1.9 MW, with a high of 85.2 MW, twelve lines having errors above 50 MW and 501 above 10 MW.

In order to compare the accuracy of the dc SCOPF, the systems were solved using the full SCOPF and the dc SCOPF respectively. Table 4 shows a comparison of the final binding constraints, with the first column showing the binding device (the binding contingency is not shown), the second column showing the marginal cost of enforcing constraints in the full SCOPF ($/MVA-hr), while the last column shows the marginal cost of enforcing the dc constraints ($/MWh).

At first glace the results for the dc SCOPF appear mixed. It was fairly effective in identifying the same binding constraints as the ac (12 out of 23) and only had one constraint not found by the ac approach. Yet, it still missed almost 50% of the binding constraints, including the constraint with the highest marginal cost. However, a more in-depth look indicates that at least some of these misses were really near misses. For example, the first constraint arises from an overload on one of three parallel 345/138 kV transformers for the contingent outage of the largest of the three. The dc approach misses this, but only by a sliver, calculating a percentage loading of 95%. The next two missed constraints, the sixth and the seventh, are both base case violations near the edge of the equivalenced system. The dc approach calculates these flows to be 98% and 99%. So again it misses, but not by much. The single dc constraint that is not included in the ac solution is also a near miss – the ac contingent flow on this device is 99%. The differences in the marginal enforcement costs are more problematic for the several constraints with high values. But such high values indicate constraints that are difficult to enforce, and can be quite sensitive to relatively minor changes in model values.

Table 4: Comparison of AC and DC Binding Constraints

Binding Device	AC Cost	DC Cost
Line from 39157 to 39167 ckt. 3	456.75	
Trans. from 25430 to 26444 ckt. 1	433.22	94.36
Line from 39215 to 39214 ckt. 1	139.02	186.94
Line from 25914 to 25913 ckt. 1	93.57	160.16
Line from 30762 to 31764 ckt. 1	90.34	76.41
Line from 22616 to 22618 ckt. 1	63.96	
Line from 26104 to 26105 ckt. 1	56.89	
Line from 39472 to 39471 ckt. 1	55.31	50.24
Line from 36362 to 36057 ckt. 1	50.25	32.93
Line from 36709 to 37395 ckt. 1	45.91	
Line from 39058 to 39059 ckt. 1	36.72	36.31
Line from 36697 to 36731 ckt. 1	34.31	
SuperArea MW Constraint	33.05	32.79
Line from 64080 to 64635 ckt. 1	32.15	32.67
Line from 28547 to 28546 ckt. 2	31.4	50.80
Line from 36922 to 36968 ckt. 1	24.66	26.37
Line from 36298 to 36027 ckt. 1	13.81	
Line from 22663 to 22686 ckt. 1	12.24	
Line from 38852 to 38851 ckt. 2	12.04	12.58
Line from 18422 to 18425 ckt. 1	6.19	2.64
Line from 36683 to 37191 ckt. 1	2.67	
Line from 36684 to 37074 ckt. 1	2.22	
Line from 36036 to 36697 ckt. 1	2.15	
Line from 36814 to 37254 ckt. 1	1.28	
Line from 64403 to 64680 ckt. 1		39.54

Concerning the LMPs, as would be expected, differences in the marginal values have a direct impact on the LMPs. Overall the average ac LMP was $38.56/MWh, while the average dc LMP was $36.13/MWh. Figure 7 shows plots of the sorted LMPs for the two solutions, while Figure 8 and Figure 9 show contours of the LMPs in the Northern Illinois region. In the figures the color change in the Quad Cities area on the Illinois/Iowa border is due to the last constraint in Table 4 being in the dc solution but not the ac solution. As was mentioned at the end of Section 2, constraints only affect the LMPs when they are actually binding; being close doesn't count. But once a constraint becomes binding, its marginal enforcement cost, and hence its impact on the LMPs at nearby buses can be significant.

In comparing solution times the dc approach was approximately 60 times faster than the ac approach. When three outer loops were required (hence, the need to solve 3*1360 = 4080 contingencies) the dc SCOPF solved in about 95 seconds, while the ac SCOPF took about 95 minutes. With the ac solution each contingency was

solved completely using a full power flow, including the calculation of all reactive controls. While the ac solution time could have been substantially decreased through the use of contingency screening techniques (with a good biography provided at the end of Chapter 11 of [6]), given the focus of this paper on accuracy, not solution time, we felt introducing approximations in the ac solution would be counterproductive.

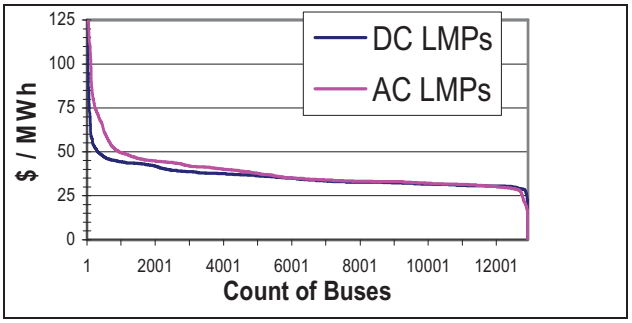

Figure 7: Sorted Bus LMPs

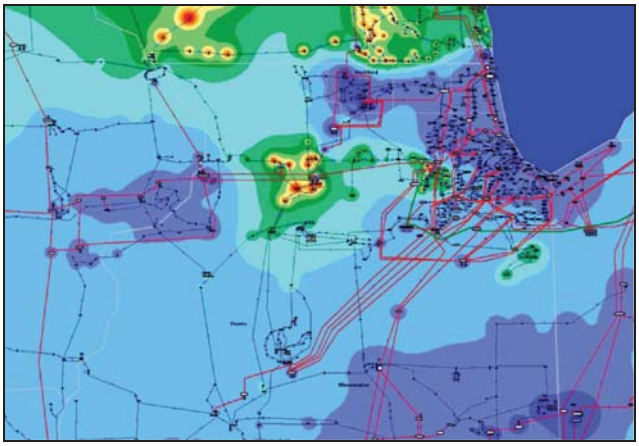

Figure 8: Contour of AC LMPs in Northern Illinois

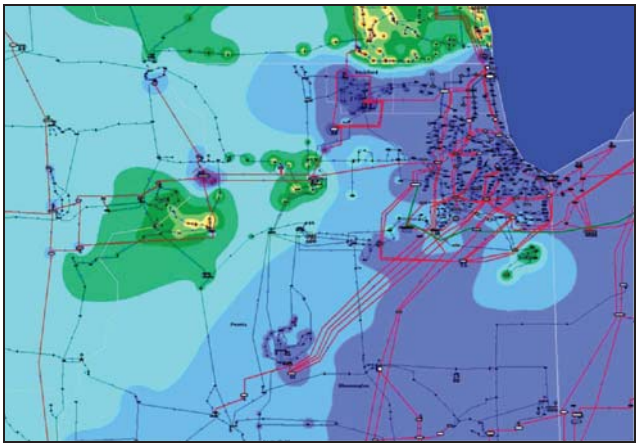

Figure 9 : Contour of DC LMPs in Northern Illinois

5. Conclusion

Overall the results of this study were quite encouraging. For the cases considered here the dc SCOPF appeared to do a fairly good job of revealing the congestion patterns that would actually occur using the full ac system models, with the key advantage that the dc approach is substantially faster. Still, there is room for improvement, and we would recommend future research to incorporate the techniques of [22] into the dc SCOPF. A comparison of such a modified dc SCOPF with the full ac approach would be of interest.

6. Acknowledgement

The authors would like to acknowledge the support of the U.S. Department of Energy through the Consortium for Electric Reliability Technology Solutions (CERTS) program, PSERC (Power System Engineering Research Center), the Grainer Foundation and PowerWorld Corporation.

7. References

[1] A. Klos, A. Kerner, “The non-uniqueness of the load flow solution,” Proc. PSCC-5, 3.1-8, Cambridge, UK, 1975.

[2] C.L. DeMarco, T.J. Overbye, “Low voltage power flow solutions and their role in exit time based security measures for voltage collapse,” *Proc. 27th Conf. Decision & Control*, Austin, TX, Dec. 1988.

[3] J.S. Thorp, S.A. Naqavi, “Load flow fractals,” *Proc. 28th Conf. Decision and Control*, Tampa, FL, Dec 1989.

[4] J.S. Thorp, S.A. Naqavi, “Load-flow fractals draw clues to erratic behavior,” *IEEE Computer Applications in Power*, Jan. 1997, pp. 59-62.

[5] R.J. Kaye, F.F. Wu, “Analysis of linearized decoupled power flow approximations for steady-state security assessment,” *IEEE Trans. Circuits and Systems*, July 1984, pp. 623-636.

[6] A.J. Wood, B.F. Wollenberg, *Power Generation, Operation and Control*, 2nd Edition, John Wiley & Sons, New York, 1996.

[7] T. J. Overbye, "A power flow measure for unsolvable cases," *IEEE Trans. on Power Systems*, vol. PWRS-9, pp. 1359-1365, August 1994.

[8] C.A. MacArthur, "Transmission limitations computed by superposition," *AIEE Trans. on Power Apparatus and Systems*, Dec. 1961, pp. 827-831.

[9] P.W. Sauer, "On the formulation of power distribution factors for linear load flow methods," *IEEE Trans. on Power Apparatus and Systems*, Feb. 1981, pp. 764-770.

[10] J. Carpienterm, “Contribution e l’étude do Dispatching Economique,” *Bulletin Society Francaise Electriciens*, Vol. 3, August 1962.

[11] H.W. Dommel, W.F. Tinney, "Optimal power flow solutions," *IEEE Trans. Power Apparatus and Sys*tems, Oct. 1968, pp. 1866-1876.
[12] A. Monticelli, M.V.F. Pereira, S. Granville, "Security constrained optimal power flow with post-contingency corrective scheduling," IEEE Trans. on Power Systems, Feb. 1987, pp. 175-182.
[13] B. Stott, O. Alsac, A.J. Monticelli, "Security analysis and optimization," *Proc. of IEEE*, Dec. 1987, pp. 1623-1644.
[14] T. Bertram, K.D. Demaree, L.C. Dangelmaier, "An integrated package for real-time security enhancement," *IEEE Trans. on Power Systems*, May 1990, pp. 592-600.
[15] J.A. Momoh, M.E. El-Hawary, R. Adapa, "A review of selected optimal power flow literature to 1993*," IEEE Trans. on Power Systems*, February 1999, pp. 96-111.
[16] M. E. El-Hawary et. al., *IEEE Tutorial Course, Optimal Power Flow: Solution Techniques, Requirements and Challenges*, IEEE 96 TP 110-0, 1996.
[17] B. Stott and J.L. Marinho, "Linear programming for power system network security applications," *IEEE Trans. on Power Apparatus and Systems*, Vol. PAS-98, May/June 1979, pp. 837-848.
[18] G.B. Dantzig, M.N. Thapa, *Linear Programming*, Springer, New York, NY, 1997.
[19] T. J. Overbye, "Estimating the actual cost of transmission system congestion," *Proc. 36th Hawaii International Conference on System Sciences*, Kona, HI, January 2003.
[20] O. Alsac, J. Bright, M. Prais, B. Stott, "Further developments in LP-based optimal power flow," *IEEE Trans. on Power Systems*, August 1990, pp. 697-711.
[21] T.J. Overbye, "Fostering intuitive minds for power system design," *P&E Magazine*, July/August 2003 [to appear].
[22] S. Grijalva, P.W. Sauer, J.D. Weber, "Enhancement of linear ATC calculations by the incorporation of reactive power flows," *IEEE. Trans. on Power Systems*, May 2003, pp. 619-624.
[23] T.J. Overbye, D.A. Wiegmann, R.J. Thomas, "Visualization of Power Systems," (Chapter 5), PSERC Report 02-36. November, 2002. Available on-line at www.pserc.wisc.edu.